THE JOURNAL OF BIOLOGICAL CHEMISTRY VOL. 282, NO. 30, pp. 21848–21855, July 27, 2007
© 2007 by The American Society for Biochemistry and Molecular Biology, Inc. Printed in the U.S.A.

Characterization of a Factor Xa Binding Site on Factor Va near the Arg-506 Activated Protein C Cleavage Site*

Received for publication, March 13, 2007, and in revised form, May 24, 2007 Published, JBC Papers in Press, June 6, 2007, DOI 10.1074/jbc.M702192200

Andrew J. Gale[‡1], **Subramanian Yegneswaran**[‡], **Xiao Xu**[‡], **Jean-Luc Pellequer**[§], **and John H. Griffin**[‡]

From the [‡]*Department of Molecular and Experimental Medicine, The Scripps Research Institute, La, Jolla, California 92037 and the* [§]*Commissariat à l'Energie Atomique Valrhô, Institute of Biotechnology and Environmental Biology, DSV/iBEB/SBTN/LIRM, 30207 Bagnols-sur Cèze, Cedex, France*

Prothrombin is proteolytically activated by the prothrombinase complex comprising the serine protease Factor (F) Xa complexed with its cofactor, FVa. Based on inhibition of the prothrombinase complex by synthetic peptides, FVa residues 493–506 were proposed as a FXa binding site. FVa is homologous to FVIIIa, the cofactor for the FIXa protease, in the FX-activating complex, and FVIIIa residues 555–561 (homologous to FVa residues 499–506) are recognized as a FIXa binding sequence. To test the hypothesis that FVa residues 499–505 contribute to FXa binding, we created the FVa loop swap mutant (designated 499–505$_{VIII}$ FV) with residues 499–505 replaced by residues 555–561 of FVIIIa, which differ at five of seven positions. Based on kinetic measurements and spectroscopic titrations, this FVa loop swap mutant had significantly reduced affinity for FXa. The fully formed prothrombinase complex containing this FVa mutant had fairly normal kinetic parameters (k_{cat} and K_m) for cleavage of prothrombin at Arg-320. However, small changes in both Arg-320 and Arg-271 cleavage rates result together in a moderate change in the pathway of prothrombin activation. Although residues 499–505 directly precede the Arg-506 cleavage site for activated protein C (APC), the 499–505$_{VIII}$ FVa mutant was inactivated entirely normally by APC. These results suggest that this A2 domain sequence of the FVa and FVIIIa cofactors evolved to have different specificity for binding FXa and FIXa while retaining compatibility as substrate for APC. In an updated three-dimensional model for the FVa structure, residues 499–505, along with Arg-506, Arg-306, and other previously suggested FXa binding sequences, delineate a continuous surface on the A2 domain that is strongly implicated as an extended FXa binding surface in the prothrombinase complex.

The prothrombinase complex is responsible for the activation of prothrombin to thrombin, the central serine protease in the coagulation pathway (1, 2). This complex is composed of the serine protease, Factor Xa (FXa),[2] with the non-enzymatic cofactor Factor Va (FVa) and forms on a phosphatidyl serine-containing membrane surface in the presence of $CaCl_2$. FXa generates thrombin via proteolysis at two sites within prothrombin. The catalytic efficiency of this reaction is increased by several orders of magnitude due to FVa (3, 4). Therefore, activation of prothrombin by FXa is most physiologically relevant in the presence of FVa.

Human FV circulates as a 330-kDa protein and is comprised of six domains, A1-A2-B-A3-C1-C2 (5). FV is activated by thrombin cleavages resulting in the release of the B domain and formation of the active heterodimer, FVa. FVa is inactivated by the anticoagulant plasma protease, activated protein C (APC), via specific proteolytic cleavages at three arginines, 306, 506, and 679 (6).

In the prothrombinase complex, FVa and FXa have extensive interactions with one another. This complex has been modeled based on the x-ray crystallographic structure of FXa and a computer-generated homology model of FVa (7). The putative interactions center on FXa binding to the A2 domain of FVa and may include sequences from 311 to 331 and from 493 to 506, which were proposed as FXa binding sites based on peptide inhibition studies (8–11). The FVa·FXa complex model suggests that the 499–505 sequence is centrally located in the binding interface (7).

FVa is highly homologous to FVIIIa, the cofactor for FIXa, the intrinsic pathway activator of FX. Therefore, it is likely that FVIIIa binds to FIXa in a complex similar to that of FVa and FXa. In fact, FVIIIa binding to FIXa also centers on the A2 domain of FVIIIa, although a sequence in the A3 domain is also involved (12, 13). In particular, FVIIIa binds to FIXa at residues 558–565 in the FVIIIa A2 domain (14, 15). This sequence in FVIII includes an APC cleavage site at Arg-562, which is homologous to the APC cleavage site in FVa at Arg-506. Therefore, this sequence in FVIIIa is homologous to residues 502–509 of FVa, which overlaps the sequence 493–506, proposed to be a FXa binding site (16). Furthermore, cleavage at Arg-506 in FVa reduces its affinity for FXa (17), whereas cleavage at Arg-562 in FVIIIa inactivates FVIIIa (18). However, the amino acid sequences immediately preceding Arg-506 in FVa and Arg-562 in FVIIIa differ in five of the seven residues (see Table 1).

* This study was supported by National Institutes of Health Grants HL82588 (to A. J. G.), HL07695 (to S. Y.), and HL21544 (to J. H. G.) and by a grant from the Sam and Rose Stein Endowment Fund and the Armstrong McDonald Foundation (to A. J. G.). The costs of publication of this article were defrayed in part by the payment of page charges. This article must therefore be hereby marked "*advertisement*" in accordance with 18 U.S.C. Section 1734 solely to indicate this fact.

[1] To whom correspondence should be addressed: Dept. of Molecular and Experimental Medicine, The Scripps Research Institute, MEM-286, 10550 N. Torrey Pines Rd., La Jolla, CA 92037. Tel.: 858-784-2177; Fax: 858-784-7981; E-mail: agale@scripps.edu.

[2] The abbreviations used are: FXa, Factor Xa; FV, Factor V; APC, activated protein C; PC, phosphatidyl choline; PS, phosphatidyl serine; LWB, light-with-a-bite; BHK, baby hamster kidney; MOPS, 4-morpholinepropanesulfonic acid; BisTris, 2-[bis(2-hydroxyethyl)amino]-2-(hydroxymethyl)propane-1,3-diol.

This is an Open Access article under the CC BY license.

Therefore, our hypothesis was that residues 499–505 in FVa contribute to FXa binding specificity in FVa, whereas both the FVa and the FVIIIa sequences support APC cleavage at Arg-506 and Arg-562, respectively. Therefore, this sequence in FVa and FVIIIa provides an important functional motif in the prothrombinase and FXase complexes that would not be interchangeable. To test this hypothesis for the prothrombinase complex, we designed and produced a loop swap mutant of FV in which we replaced the sequence of 499–505 of FV with the sequence of 555–561 of FVIII (499–505_{VIII} FV, see Table 1). When we measured prothrombinase function and direct binding of FXa to FVa, we found that this FVa mutant had greatly reduced affinity for FXa but that when it was fully incorporated into the prothrombinase complex, it exhibited near normal prothrombinase activity. Additionally, this FVa mutant was normally inactivated by APC. The data support our hypotheses and provide experimental evidence that supports elements of a previous model of the prothrombinase complex (7).

MATERIALS AND METHODS

Proteins and Reagents—Protein S, FXa, and Gla-domainless β FXa were purchased from Hematologic Technologies (Essex Junction, VT). Prothrombin and APC were purchased from Enzyme Research Laboratories (South Bend, IN). Phospholipid vesicles (80% phosphatidyl choline, 20% phosphatidyl serine) were prepared as described from phosphatidyl choline (PC) purchased from Avanti Polar Lipids (Alabaster, AL), and phosphatidyl serine (PS) was purchased from Sigma-Aldrich (19). The chromogenic substrate H-D-CHG-Ala-Arg-pNA (where CHG indicates cyclohexylglycine and pNA indicates paranitroanilide) (Pefachrome TH) was purchased from Centerchem, Inc. (Norwalk, CT).

Expression and Purification of Recombinant Factor V—The Factor V loop swap mutant (499–505_{VIII} FV, see Table 1) was made in the background of B domain-deleted FV with a mutation of Ser-2183 to Ala to remove a carbohydrate attachment site that is incompletely utilized to generate a more homogenous protein (20). Throughout this report, 2183A B domain-deleted FV will be referred to as wild type FV. Mutagenesis was performed with a Stratagene QuikChange mutagenesis kit, and the mutant sequence was confirmed by sequencing in the Departmental DNA core at The Scripps Research Institute. The B domain-deleted FV gene was inserted into the pED plasmid (21) and co-transfected with the plasmid pRSVneo, for selection with geneticin, into modified BHK cells (a gift from Rodney Camire, Philadelphia, PA). FV was purified from conditioned medium as described (20) except that, instead of polyethylene glycol 6000 precipitation, the conditioned medium was loaded onto an anti-heavy chain FV monoclonal antibody affinity column (3B1-Sepharose) (22) equilibrated with 50 mM Tris, 100 mM NaCl, 0.05% NaN_3, pH 7.4, and then eluted with a gradient up to 2 M NaCl. FV eluted from that column was then purified on an anti-light chain FV monoclonal antibody column as described (20) (AHV5101-Sepharose, AHV5101 from Hematologic Technologies). FV was activated with thrombin (200 ng/ml) for 20 min at 37 °C, and the thrombin was inactivated with a slight excess of hirudin. FVa was quantified by enzyme-linked immunosorbent assay as described (20). FV and FVa purity were evaluated by SDS-PAGE analysis with 4–12% Bis-Tris gels with MOPS-SDS buffer (Invitrogen) stained with Simply Blue Safestain (Invitrogen).

Functional Assays—We determined the functional properties (FXa binding, K_m, and k_{cat} for prothrombin) in prothrombinase complex assays with purified components. In brief, aliquots of FVa in 50 mM HEPES, 150 mM NaCl, 5 mM $CaCl_2$, 0.1 mM $MnCl_2$, 0.5% bovine serum albumin, and 0.05% NaN_3 (prothrombinase buffer) containing phospholipid vesicles (unless otherwise noted) were dispensed into wells of a 96-well plate. At defined times, FXa was added to each well, immediately followed by prothrombin. After 3 min, the prothrombinase reaction was stopped with EDTA, and then the thrombin substrate Pefachrome TH was added, and the cleavage rate was monitored on a Molecular Devices Versamax plate reader. The data were converted to thrombin concentration with a standard curve of α-thrombin in the same assay.

For these assays, functional FVa concentration was determined by analysis of two titration curves, one of FVa and one of FXa, into the prothrombinase reaction. A very similar protocol was already described for FVIIIa and FIXa and was used here (23, 24). For the FVa titration, FXa was fixed at 5 pM, prothrombin was fixed at 0.86 μM, and FVa was varied from 2 to 256 pM. For the FXa titrations, FVa was fixed at around 3 pM, prothrombin was fixed at 0.86 μM, and FXa was varied from 2 to 256 pM. Actual functional concentration of FVa in the prothrombinase complex was calculated as described (24), and then in subsequent assays, FVa was fixed at 2.8 pM based on that calculation. For prothrombin titrations, FXa was the limiting component of the prothrombinase complex (2 pM), whereas FVa was in excess (250 pM). Prothrombin was titrated from 0.023 to 1.5 μM. Gla-domainless FXa was titrated from 1.56 to 200 nM in the absence of phospholipid vesicles with 200 pM FVa and 5.7 μM prothrombin. For FXa titrations, data from a control titration without FVa present were subtracted out of each titration to distinguish FVa-dependent from FVa-independent prothrombin activation. K_m and V_{max} were determined from a hyperbolic curve fit, and k_{cat} was calculated using the concentration of the prothrombinase complex, which was determined based on the derived $K_{½}$ and the concentrations of FXa and FVa. Therefore, for wild type FVa, the prothrombinase concentration was 1.95 pM when FXa was 2 pM and FVa was 250 pM, whereas for 499–505_{VIII} FVa, with a $K_{½}$ of 130 pM, the prothrombinase concentration was 1.32 pM when FXa was 2 pM and FVa was 250 pM.

APC inactivation time courses with APC or with APC and protein S were performed with 0.55 nM FVa and the concentrations of APC and protein S given in the legend for Fig. 5. For inactivation time courses in the presence of FXa, FXa was included at 1 nM during the APC and FVa incubation and was also 1 nM during the final assay of remaining FVa activity in the prothrombinase assay. This assay was performed essentially as described, and inactivation curves were fit to a double exponential decay (25). Apparent second order rate constants in units of $M^{-1}s^{-1}$ were derived from these curve fits.

Gel Analysis of Prothrombin Cleavage—Prothrombin at 5 μM was incubated at room temperature with 0.2 nM FXa, 2 nM FVa, and 25 μM phospholipid vesicles in prothrombinase buffer lacking bovine serum albumin. A zero time aliquot was removed

right before the addition of FXa, and then further aliquots were removed and quenched in protein gel sample buffer containing 2 mg/ml dithiothreitol and 20 mM EDTA at the indicated time points (minutes). After reduction and denaturation, samples were alkylated with iodoacetamide to prevent reoxidation. Samples were run on a 4–12% BisTris gel with MOPS-SDS buffer (Invitrogen) with antioxidant present. Densitometry was performed with Unscan-It (Silk Scientific, Orem, UT). Staining intensity was corrected for background and normalized to the total corrected staining intensity for each lane. Data are presented as the fractional intensity of the theoretical maximum for each fragment.

Preparation of Active Site Labeled Factor Xa—Factor Xa was active site-specifically labeled and inhibited with light-with-a-bite (LWB) attached to Phe-Pro-Arg-chloromethyl ketone, and then the labeled protein was purified from the excess reactants according to procedures described previously (26). LWB is a multicomponent fluorescent probe that was designed and synthesized in-house (26–28). The fluorescent component of LWB is a fluorescein (Fl) dye, and so LWB-labeled FXa_i is referred to as Fl-FXa_i and is sensitive to the assembly of the prothrombinase complex.

Fluorescence Binding Assays—Fluorescence binding assays were performed essentially as described (26, 28). Briefly, for these assays, two samples were prepared in parallel. The sample cuvette received 9.4 nM of Fl-FXa_i in 50 mM HEPES, 150 mM NaCl, 5 mM $CaCl_2$, whereas the blank cuvette received an equal concentration of non-fluorescent active site-inhibited FFR-FXa_i (FXa inhibited by D-Phe-Phe-Arg-CH_2Cl, Calbiochem) in the same buffer. The initial net fluorescence intensity of the sample, designated F_o, was obtained by subtraction of a dye-free blank cuvette from the sample cuvette signal. Upon titration of PC/PS (4:1 w/w) vesicles, the net-dilution corrected fluorescence intensity (F) of Fl-FXa_i decreased and reached a plateau at ~25 μM lipid. At this point in the titration, wild type FVa or 499–505_{VIII} FVa was titrated into the cuvette. Dissociation constants were derived from fit to a quadratic equation as described (29, 30).

FVa Model—Human FVa was modeled based on the crystal structure of the inactivated bovine FVa (Protein Data Bank code 1SDD) (31) and our previously modeled human FVa A domains trimer based on ceruloplasmin (32). This previous model was used to fill in missing loops and the missing A2 domain from the crystal structure. After humanization of the bovine FVa side chains, missing loops were built by superimposing the previous human FVa model onto the humanized bovine FVa using two overlapping residues on each side of the loop. All replaced side chains were optimized (33) then Cartesian coordinates of all atoms were energy-minimized with X-PLOR using standard protocols (32).

RESULTS

Preparation and Characterization of Recombinant FV—FV and FVIII were aligned according to Kane and Davie (16), and we observed significant differences between their sequences at the proposed FXa binding site before the APC cleavage site at Arg-506 in FVa (Table 1) (9). Given that FXa does not utilize FVIIIa as a cofactor, it seemed reasonable that insertion of FVIII sequence might abrogate the FXa binding site while retaining the native fold of the A2 domain. We mutated five residues between amino acids 499 and 505 in FV (Table 1, mutant 499–505_{VIII} FV) to generate the homologous sequence present in FVIII. Sequencing of the plasmid and of DNA purified from stably transfected cells confirmed the mutations. FV variants were purified from medium collected from stably transfected BHK cells and assayed for concentration by enzyme-linked immunosorbent assay of thrombin-activated FVa as described (20). This process resulted in much higher levels of expression than previously obtained in COS cells, due to improved expression in BHK cells. Yields ranged from 100 to 600 μg of pure protein/liter of starting medium. Coomassie Blue-stained SDS-PAGE suggested that the proteins were about 90% pure (Fig. 1).

TABLE 1

Alignment of factor V and factor VIII at the loop preceding the APC cleavage site and the sequence of the homologous loop swap mutant

Bold underline indicates the loop swap.

Factor	Sequence
Factor V	495-LLIC**KSRSLDR**RGIQ-509
Factor VIII	551-LLIC**YKESVDQ**RGNQ-565
499–505_{VIII} FV	499-KSRSLDR-505 → 499-**YKE**S**V**D**Q**-505

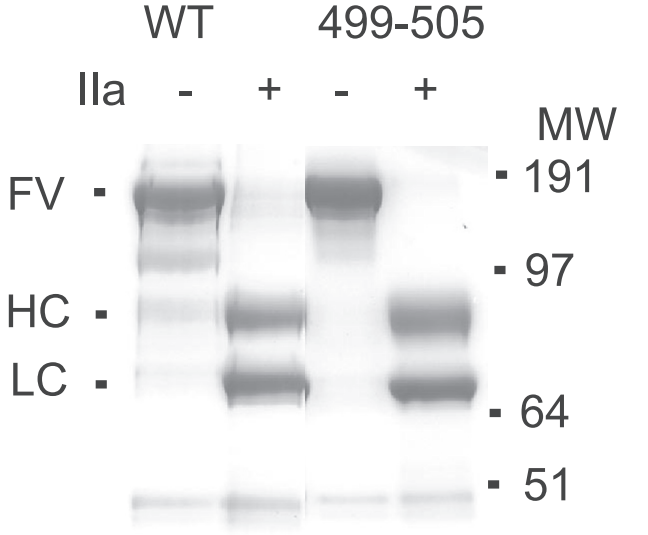

FIGURE 1. **SDS-PAGE of purified FV variants.** Approximately 5 μg of reduced FV was loaded per lane either as FV or as FVa after reaction with 0.2 μg/ml thrombin at 37 °C for 20 min. Gels were stained with Simply Blue Safestain. Molecular weight markers (*MW*) in kDa are listed on the *right*. *HC* = heavy chain; *LC* = light chain; *IIa* = α-thrombin. *WT*, wild type.

Functional Properties of FVa Variants—We then determined the relative affinity of the loop swap mutant 499–505_{VIII} FVa and wild type FVa for FXa in an assay of the prothrombinase complex by titrating FXa into the prothrombinase assay (Fig. 2*A*). A hyperbolic curve fit gave $K_{½}$, the functional K_d in the prothrombinase complex. Mutant 499–505_{VIII} FVa had greatly reduced affinity for FXa in the prothrombinase complex ($K_{½}$ = 130 pM when compared with 6.4 pM for wild type FVa, Table 2). We also titrated the substrate, prothrombin, into the prothrombinase complex reaction to determine K_m and k_{cat} for prothrombin cleavage. This assay monitors Arg-320 cleavage only since only that cleavage is required to generate amidolytic

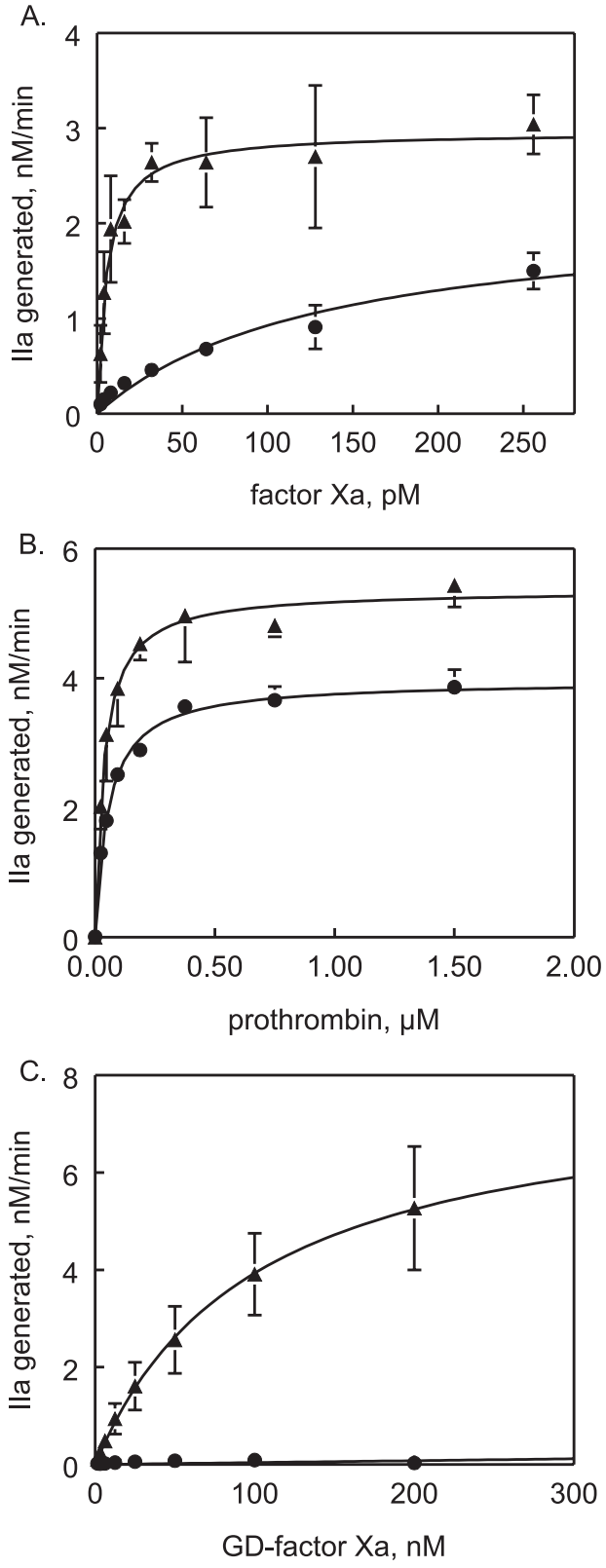

FIGURE 2. **499–505$_{VIII}$ FVa has altered functional properties in the purified prothrombinase complex.** *A*, FXa was titrated into the prothrombinase complex as described. An apparent K_d ($K_{1/2}$) for FVa and FXa in the prothrombinase complex was derived from the hyperbolic curve fit of these data (Table 2). *B*, prothrombin was titrated into the prothrombinase complex, and the K_m and k_{cat} values for the prothrombinase complex composed of normal FXa and either of the two FVa variants were derived from the hyperbolic curve fit with k_{cat} adjusted for the fraction of FXa bound in the prothrombinase complex with the respective FVa variant. *C*, Gla-domainless FXa was titrated into the prothrombinase complex in the absence of phospholipid to isolate the FVa-FXa protein-protein interactions, and an apparent K_d ($K_{1/2}$) was derived from the hyperbolic curve fit. ▲ = wild type FVa; ● = 499–505$_{VIII}$ FVa. All curves are the averages of 3–4 experiments, and *error bars* show standard deviation.

TABLE 2

Kinetic parameters of FVa variants in the prothrombinase complex in the presence or absence of phospholipid vesicles

Assays were performed with phospholipid vesicles present except for Gla-domainless-β-factor Xa. (GD-Xa). II = prothrombin; ND = not detectable.

	$K_{1/2}$, Xa	K_m, II	k_{cat}, II	$K_{1/2}$, GD-Xa
	pM	*nM*	s^{-1}	*nM*
Wild type FVa	6.4 ± 3.5	39 ± 15	46 ± 1	104 ± 23
499–505$_{VIII}$ FVa	130 ± 64	55 ± 4	50 ± 2	ND

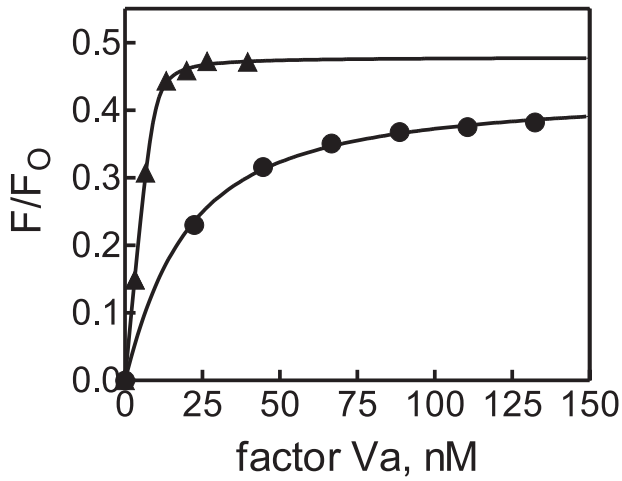

FIGURE 3. **499–505$_{VIII}$ FVa binds with greatly reduced affinity to Fl-FXa.** FVa was titrated into Fl-FXa$_i$, and fluorescence intensity change was monitored. ▲ = wild type FVa; ● = 499–505$_{VIII}$ FVa. Data were fit to a quadratic equation from which the K_d was derived. Standard deviations were too small to be visible on this graph.

activity in thrombin. The prothrombinase complex containing 499–505$_{VIII}$ FVa had kinetic properties for prothrombin cleavage that were similar to those observed with wild type FVa (Fig. 2*B* and Table 2). Therefore, mutation of residues 499–505 in FVa greatly decreased affinity for FXa but had only small effects on the rate of cleavage of Arg-320 by the resulting prothrombinase complex when it did form.

To confirm that the loss in FXa affinity was not due to some alteration of phospholipid binding, we replaced FXa with Gla-domainless FXa in an assay of the prothrombinase complex without phospholipid present. The $K_{1/2}$ of wild type FVa for Gla-domainless FXa was 104 nM, whereas no binding was detectable at all for 499–505$_{VIII}$ FVa, confirming that 499–505$_{VIII}$ FVa had greatly reduced affinity for FXa in the absence or presence of phospholipid (Fig. 2*C* and Table 2).

Binding of Fl-FXa$_i$ to Factor Va—To characterize directly the binding of 499–505$_{VIII}$ FVa to FXa, we measured binding of FVa to Fl-FXa$_i$ in the presence of PC/PS vesicles monitored with a fluorescence spectrophotometer. The fluorescence intensity of the PC/PS-bound Fl-FXa$_i$ typically increased by ~47% when wild type FVa was titrated (Fig. 3, *triangles*) and reached a plateau at ~13 nM FVa, suggesting a 1:1 stoichiometry for the FXa-FVa complex on PC/PS vesicles. The curve fit to a quadratic equation returned a K_d of 0.4 nM, a value identical to

other results for recombinant FVa (34). When PC/PS-bound Fl-FXa$_i$ was titrated with 499–505$_{VIII}$ FVa, the fluorescence intensity increased less sharply when compared with wild type FVa (Fig. 3, *circles*). The curve fit to a quadratic equation returned a K_d of 14.2 nM. Thus, the loop swap reduced the affinity of FVa for FXa by ~35-fold in direct binding assays. These K_d values were much larger than those determined in the functional assay because the third protein in the prothrombinase complex, prothrombin, was not present. A comparable difference in affinity was measured when prothrombin was titrated against Fl-FXa in the absence or presence of FVa (26). The reduction in apparent affinity for FXa due to the loop swap mutation was very similar, 20–35-fold, in both kinetic studies and direct binding studies. Thus, the loop swap mutation reduced affinity of FXa for FVa.

Cleavage of Prothrombin—The kinetic properties of the prothrombinase complex formed with wild type or 499–505$_{VIII}$ FVa determined in Fig. 2 monitored amidolytic activity of thrombin toward a tripeptide substrate as enzyme activity readout. Thus, these assays essentially assayed cleavage only at Arg-320 since that cleavage alone generates the full amidolytic activity derived from prothrombin. However, full generation of fully procoagulant thrombin (α-thrombin) requires cleavage at Arg-271 and Arg-320. To monitor both cleavages, we performed digests of prothrombin with FXa in the presence of phospholipid and either wild type FVa or 499–505$_{VIII}$ FVa (Fig. 4). FVa was in significant excess so that essentially all the FXa would be bound to FVa in the prothrombinase complex. In *panel A*, it is clear that the decrease in intensity of the prothrombin band, which would be due to either cleavage, was similar for both FVa variants. However, the distribution of resulting prothrombin fragments was somewhat different although qualitatively similar.

Fig. 4, *B* and *C*, shows the fractional prothrombin fragment concentrations for the wild type FVa and 499–505$_{VIII}$ FVa reactions. As expected, with wild type FVa, FXa cleaved prothrombin faster at Arg-320 than at Arg-271 (Fig. 4*B*). This resulted in fast production of fragment IIaB (residues 321–579, *inverted triangle*) and virtually no accumulation of fragment Pre2 (residues 272–579, *diamonds*). There was an apparent lag in cleavage at Arg-271, resulting in a lag in accumulation of fragment F1.2 (residues 1–271, *triangles*). This rate increased over time, however, resulting in fairly high accumulation of F1.2 by the end of the time course.

The fractional accumulation of the various prothrombin fragments in the presence of 499–505$_{VIII}$ FVa was moderately but reproducibly different (Fig. 4*C*). Cleavage at Arg-320 was somewhat slowed, resulting in a moderate decrease in the rate of IIaB accumulation (320–579, inverted triangles). However, it appeared that cleavage at Arg-271 was somewhat increased at early time points, resulting in noticeable accumulation of the Pre2 fragment (272–579, *diamonds*) and steady accumulation of the F1.2 fragment (1–271, *triangles*) rather than an early lag. As a result, F1.2-A (1–320, *circles*) and IIaB (320–579, *inverted triangles*) accumulations were somewhat lower. Thus, the prothrombinase complex formed with 499–505$_{VIII}$ FVa did have moderate changes in cleavage rates relative to wild type FVa.

Inactivation of FVa by APC—We measured the inactivation of wild type and mutant FVa by APC alone or APC in the presence of protein S (Fig. 5). APC cleaves both FVa and FVIIIa; thus it may interact similarly with both the FVa wild type and the FVIIIa homologous loop sequences in FVa. 499–505$_{VIII}$ FVa was

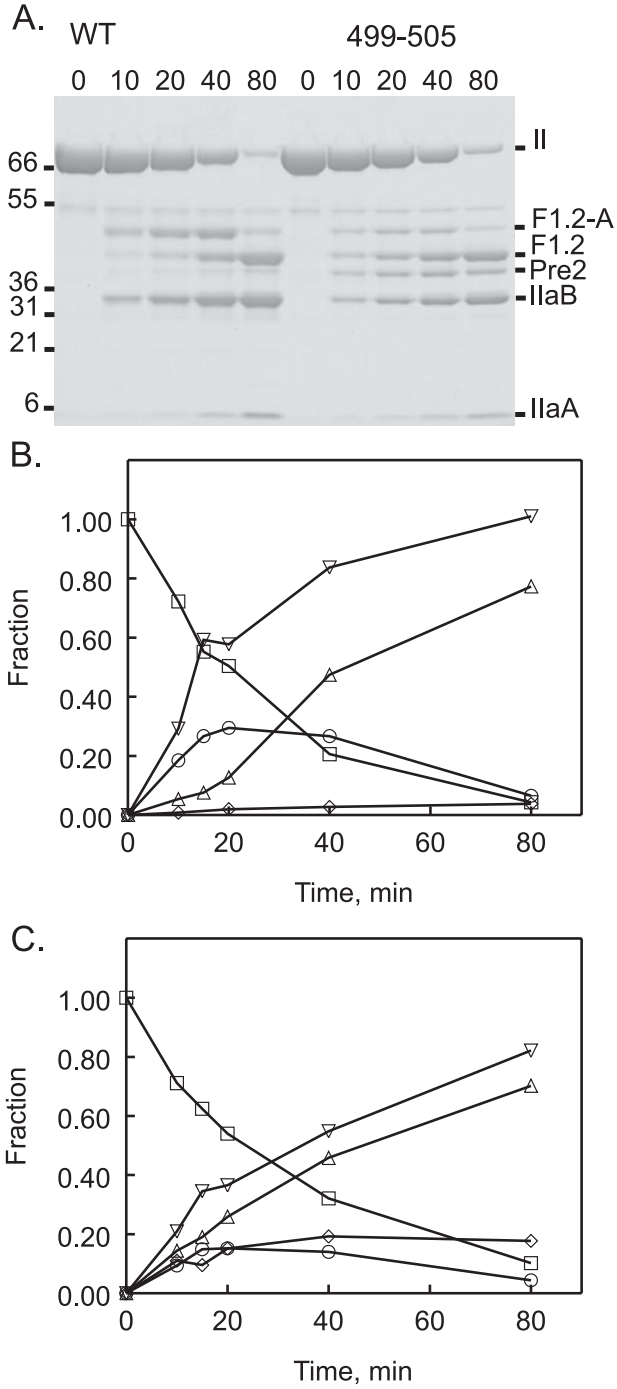

FIGURE 4. **Cleavage of prothrombin by the prothrombinase complex containing wild type FVa or 499–505$_{VIII}$ FVa.** *A*, reduced Coomassie Blue-stained gel of a time course, in minutes, of prothrombin cleavage. The cleavage reactions are described under "Materials and Methods." Samples were reduced with dithiothreitol, alkylated with iodoacetamide, and run on a 4–12% BisTris gel with MOPS-SDS buffer from Invitrogen. Molecular weight standards are indicated on the *left*, and prothrombin fragment identifications are indicated on the *right*. *II* = intact prothrombin; *F1.2-A* = amino acids 1–320; *F1.2* = amino acids 1–271; *Pre2* = amino acids 272–579; *IIaB* = amino acids 321–579; and *IIaA* = amino acids 272–320. *B* and *C*, quantitative densitometry of wild type FVa (*B*) and 499–505$_{VIII}$ FVa (*C*) from the gel in *panel A*. The *y* axis is the fraction of the maximum possible fragment concentration. □ = II; ○ = F1.2-A; △ = F1.2; ◇ = Pre2; and ▽ = IIaB. Results are combined from 2 different experiments.

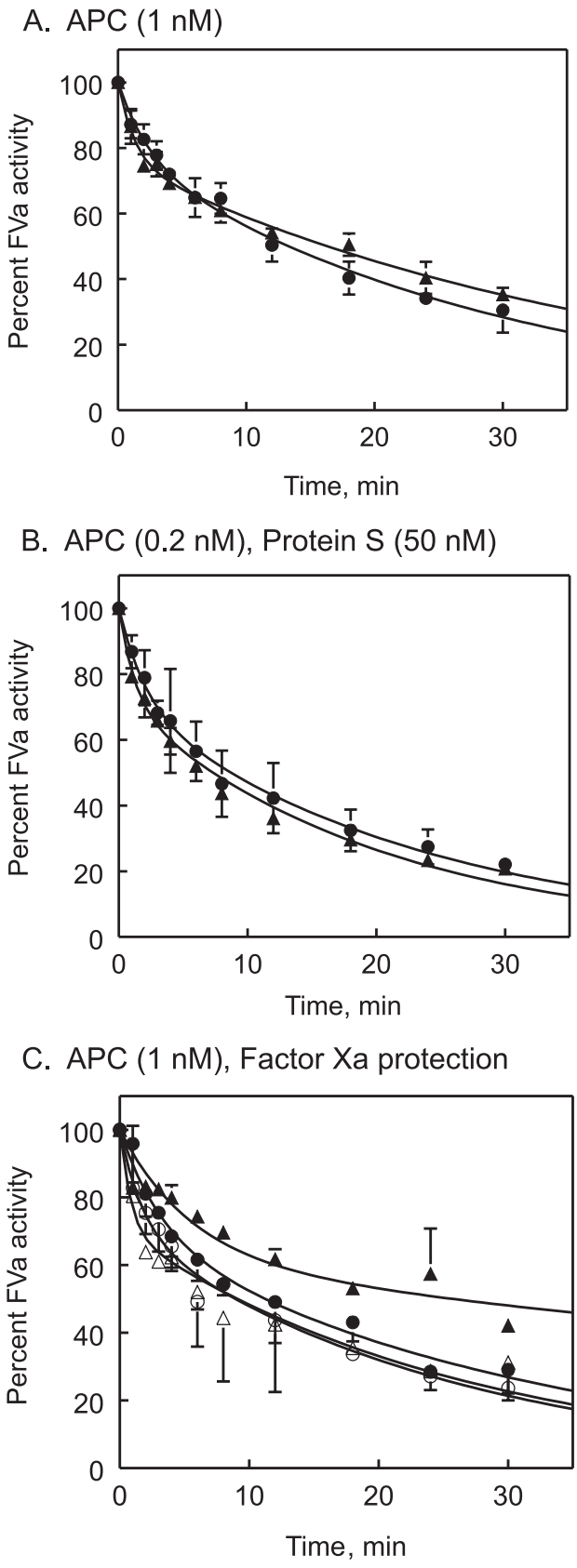

FIGURE 5. **499–505$_{VIII}$ FVa is inactivated by APC essentially the same as wild type FVa.** *A*, inactivation of FVa variants over time by 1 nM APC alone as described under "Materials and Methods." ▲ = wild type FVa; ● = 499–505$_{VIII}$ FVa. *B*, inactivation of FVa variants over time by 0.2 nM APC and 50 nM protein S as described under "Materials and Methods." ▲ = wild type FVa; ● = 499–505$_{VIII}$ FVa. *C*, inactivation of FVa variants by 1 nM APC in the absence or presence of 1 nM FXa as described under "Materials and Methods." △, ▲ = wild type FVa; ○, ● = 499–505$_{VIII}$ FVa. *Closed symbols* are in the presence of 1 nM FXa. Curves are the averages of 2–4 experiments, and *error bars* show standard deviation.

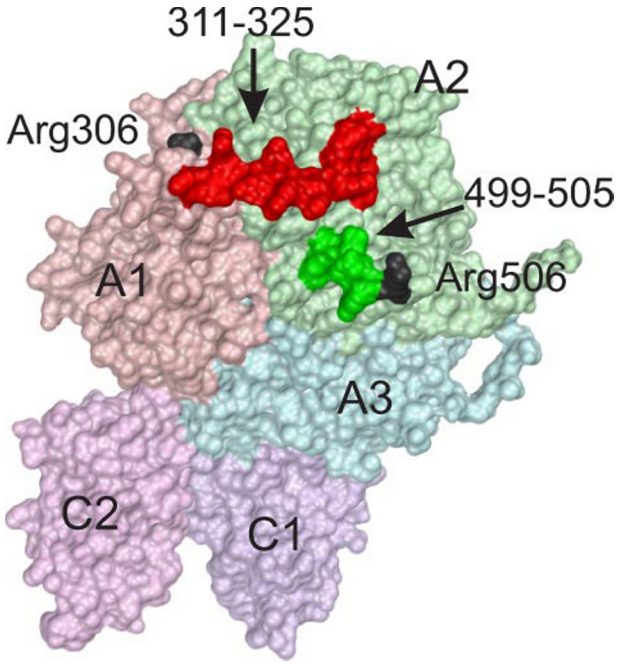

FIGURE 6. **Model of human FVa based on the crystal structure of bovine inactivated FVa.** The model included amino acids 1–663 of the heavy chain and 1546–2196 of the light chain. From the N terminus to the C terminus, the A1 domain is *pink*, A2 is *light green*, A3 is *blue*, C1 is *purple*, and C2 is *magenta*. Arg-306 and Arg-506 are *black*, residues 311–325 are *red*, and residues 499–505 are *dark green*. The figure was created with PMV v1.4.4 (44).

inactivated by APC at a very similar rate as wild type FVa both in the presence and in the absence of protein S.

FXa protects FVa from APC cleavage (35). Since 499–505$_{VIII}$ FVa has reduced affinity for FXa, this protection should be less apparent for the loop swap mutant. We tested this using the same assay conditions as Fig. 5*A*, except that 1 nM FXa was added to the reaction of APC with FVa. Fig. 5*C* shows the inactivation time courses in the absence (*open symbols*) and presence (*closed symbols*) of 1 nM FXa for both wild type FVa and 499–505$_{VIII}$ FVa. Clearly, FXa protected wild type FVa from APC inactivation (*closed triangles*), but it did not protect 499–505$_{VIII}$ FVa (*closed circles*).

Modeling of FV-FXa Binding Motif—We built an updated model of human FVa using the crystal structure of inactivated bovine FVa for the structure of the A1, A3, C1, and C2 domains (31) and our previous human FVa model that was based on ceruloplasmin for the structure of the A2 domain (Fig. 6) (32). The new model of human FVa (Fig. 6) contained residues 1–663 of the heavy chain and the entire light chain (1546–2196). The C-terminal tail of the A2 domain (664–709) was missing in this model because it could not be modeled based on ceruloplasmin (32). Our model placed the sequence 499–505 on the surface, adjacent to the APC cleavage site at Arg-506–Gly-507. Given the large effect of mutations in the 499–505 sequence (Fig. 6, *dark green*), it is clear that this sequence is centrally involved in the FXa binding site. We also highlight

residues 311–325 (Fig. 6, *red*), which we previously demonstrated are involved in FXa binding (8).

DISCUSSION

Here we directly demonstrate that the surface loop from Lys-499 to Arg-505 of FVa is part of the extended binding site on FVa for FXa. A previous study first raised this possibility based primarily on indirect studies in which the FVa·FXa interaction was inhibited by a short synthetic peptide that included this sequence (9). The homologous loop swap mutant 499–505$_{VIII}$ FVa binds to FXa with a 20–35-fold larger K_d as measured both in assays of prothrombinase complex function and in direct binding to a fluorescent-labeled derivative of FXa. This 499–505 sequence is primarily involved in FXa binding, although it may have a minor effect on prothrombinase conformation as the kinetic parameters of the formed prothrombinase complex, *i.e.* K_m and k_{cat} for Arg-320 cleavage, were near normal, but the overall cleavage patterns for both Arg-271 and Arg-320 together were moderately affected. Furthermore, switching this 499–505 sequence of FVa to the FVIIIa sequence did not significantly impact APC proteolysis of the variant FVa, suggesting that both the FVa and the FVIIIa sequences similarly support APC cleavage at Arg-506 in FVa.

One reason we used a homologous loop swap mutagenesis approach to probe the FVa·FXa binding site is that homologous proteins have similar three-dimensional structures; therefore, homologous sequence substitutions are less likely to disrupt the native structure of the protein (36, 37). This approach is only appropriate to probe a binding interaction that is unique to the homologue being studied, in this case binding of FVa to FXa. However, it would not be informative in the case of an interaction that is common to the two homologues. Thus, in this study, we did not expect this mutation to have a large impact on the interaction of APC with FVa since APC also cleaves FVIIIa at the homologous site (38). This is, in fact, what we observed, suggesting that this sequence has evolved to have different specificity for the cofactor functions of FVa and FVIIIa while retaining similar specificity as a substrate for APC. However, a negative result (no effect on APC proteolysis), although suggestive, does not prove the hypothesis that the sequences evolved to have similar specificities as substrates for APC. Further confirmation that both sequences are compatible with efficient APC cleavage would be provided by analysis of the complementary FVIII mutant in which the FV sequence is inserted into FVIII. This would be an interesting analysis to do in the future. Such analysis would also confirm that this sequence is involved in formation of the FXase complex of FVIIIa and FIXa, which has already been demonstrated in other studies (14, 15).

Another advantage of homologous loop swap mutagenesis is that mutagenesis is certainly more sensitive than probing binding sites using monoclonal antibodies or site-directed glycosylation (7, 39) since such probes can potentially inhibit binding based only on steric hindrance. Homologous loop swap mutagenesis also has the advantage over probing with short synthetic peptides in that a short peptide may not be in a native conformation. Therefore, this study strengthens the conclusions of previous studies that this region is involved in FXa binding (9).

Models of the prothrombinase complex were recently generated using a combination of computational docking algorithms and analysis taking into account published experimental data (7). Our own model of FVa presented here and our experimental data are in agreement with previous models. In Fig. 6, we also highlight residues 311–325, which we previously identified as an FXa-interacting site based on inhibition by a synthetic peptide (8). It is clear that these sequences are quite near to each other in the FVa structure and basically form a continuous surface. The published model of the FVa·FXa complex suggests an extensive interaction between FVa and FXa, with the 499–505 sequence centrally located in the extended binding site (7). At least part of the 311–325 sequence is also close to FXa in this model. Other FVa residues proposed to be involved in FXa binding are also close to FXa in this model (10, 11, 39), but in the interests of clarity, we have not included all of these sequences in this figure.

It is interesting that the FXa binding site depicted in Fig. 6 encompasses residues near to the Arg-306 and the Arg-506 APC cleavage sites that inactivate FVa. This model of the binding site explains how FXa protects Arg-506 in FVa from APC cleavage (40), whereas APC cleavages at Arg-506 and Arg-306 each reduce the affinity of FVa for FXa (17, 20). Our data showing a lack of FXa protection from APC by 499–505$_{VIII}$ FVa, in contrast to wild type FVa, support this model (Fig. 5*C*). Since the purpose of APC proteolysis is to inactivate FVa, it is not surprising that these cleavages take place within the FVa·FXa binding motif with consequent disruption of this FXa binding site (20).

The mechanism for the moderate change in the prothrombin activation pathway is not clear. One possibility could be that this region of FVa interacts specifically with prothrombin and that this interaction is slightly altered in the mutant, as has been suggested for other FVa sequences (41). This seems unlikely since it seems clear that the 499–505 sequence interacts specifically with FXa. More likely, the reduced affinity for FXa results in a prothrombinase complex with a slightly altered conformation that somewhat differentially interacts with Arg-271 and Arg-320. Our cleavage analysis with wild type prothrombin cannot differentiate with high resolution between cleavage at Arg-271 before or after Arg-320 cleavage or between cleavage at Arg-320 before or after Arg-271 cleavage. Thus, we cannot differentiate between different models of prothrombinase interaction that postulate changes in prothrombinase conformation for the two different cleavages (42) or changes in prothrombin conformation (43). Further, based on our data, we cannot speculate on the exact nature of any conformational change of the prothrombinase complex.

In summary, the sequence of 499–505 in FVa provides a significant FXa binding motif. However, changing this sequence to the homologous sequence from FVIII does not affect APC proteolysis despite an alteration of residues directly adjacent to the APC cleavage site at Arg-506.

Acknowledgments—We are grateful to Dr. Rodney Camire (University of Pennsylvania) for the gift of BHK cells and to Diana Rozenshteyn for technical assistance.

REFERENCES

1. Mann, K. G., Butenas, S., and Brummel, K. (2003) *Arterioscler. Thromb. Vasc. Biol.* **23,** 17–25
2. Walsh, P. N., and Ahmad, S. S. (2002) *Essays Biochem.* **38,** 95–111
3. Nesheim, M. E., Taswell, J. B., and Mann, K. G. (1979) *J. Biol. Chem.* **254,** 10952–10962
4. Rosing, J., Tans, G., Govers-Riemslag, J. W. P., Zwaal, R. F. A., and Hemker, H. C. (1980) *J. Biol. Chem.* **255,** 274–283
5. Jenny, R. J., Pittman, D. D., Toole, J. J., Kriz, R. W., Aldape, R. A., Hewick, R. M., Kaufman, R. J., and Mann, K. G. (1987) *Proc. Natl. Acad. Sci. U. S. A.* **84,** 4846–4850
6. Kalafatis, M., Rand, M. D., and Mann, K. G. (1994) *J. Biol. Chem.* **269,** 31869–31880
7. Autin, L., Steen, M., Dahlback, B., and Villoutreix, B. O. (2006) *Proteins* **63,** 440–450
8. Kojima, Y., Heeb, M. J., Gale, A. J., Hackeng, T. M., and Griffin, J. H. (1998) *J. Biol. Chem.* **273,** 14900–14905
9. Heeb, M. J., Kojima, Y., Hackeng, T. M., and Griffin, J. H. (1996) *Protein Sci.* **5,** 1883–1889
10. Singh, L. S., Bukys, M. A., Beck, D. O., and Kalafatis, M. (2003) *J. Biol. Chem.* **278,** 28335–28345
11. Kalafatis, M., and Beck, D. O. (2002) *Biochemistry* **41,** 12715–12728
12. Lenting, P. J., van de Loo, J. W., Donath, M. J., van Mourik, J. A., and Mertens, K. (1996) *J. Biol. Chem.* **271,** 1935–1940
13. Fay, P. J., and Jenkins, P. V. (2005) *Blood Rev.* **19,** 15–27
14. Fay, P. J., Beattie, T., Huggins, C. F., and Regan, L. M. (1994) *J. Biol. Chem.* **269,** 20522–20527
15. Jenkins, P. V., Freas, J., Schmidt, K. M., Zhou, Q., and Fay, P. J. (2002) *Blood* **100,** 501–508
16. Kane, W. H., and Davie, E. W. (1988) *Blood* **71,** 539–555
17. Nicolaes, G. A. F., Tans, G., Thomassen, M. C. L. G. D., Hemker, H. C., Pabinger, I., Varadi, K., Schwarz, H. P., and Rosing, J. (1995) *J. Biol. Chem.* **270,** 21158–21166
18. Varfaj, F., Neuberg, J., Jenkins, P. V., Wakabayashi, H., and Fay, P. J. (2006) *Biochem. J.* **396,** 355–362
19. Mesters, R. M., Houghten, R. A., and Griffin, J. H. (1991) *J. Biol. Chem.* **266,** 24514–24519
20. Gale, A. J., Xu, X., Pellequer, J. L., Getzoff, E. D., and Griffin, J. H. (2002) *Protein Sci.* **11,** 2091–2101
21. Kaufman, R. J., Davies, M. V., Wasley, L. C., and Michnick, D. (1991) *Nucleic Acids Res.* **19,** 4485–4490
22. Heeb, M. J., Rehemtulla, A., Moussalli, M., Kojima, Y., and Kaufman, R. J. (1999) *Eur. J. Biochem.* **260,** 64–75
23. Mathur, A., Zhong, D., Sabharwal, A. K., Smith, K. J., and Bajaj, S. P. (1997) *J. Biol. Chem.* **272,** 23418–23426
24. Gale, A. J., Radtke, K. P., Cunningham, M. A., Chamberlain, D., Pellequer, J. L., and Griffin, J. H. (2006) *J. Thromb. Haemostasis* **4,** 1315–1322
25. Gale, A. J., Heeb, M. J., and Griffin, J. H. (2000) *Blood* **96,** 585–593
26. Yegneswaran, S., Fernandez, J. A., Griffin, J. H., and Dawson, P. E. (2002) *Chem. Biol.* **9,** 485–494
27. Yegneswaran, S., Mesters, R. M., Fernandez, J. A., and Griffin, J. H. (2004) *J. Biol. Chem.* **279,** 49019–49025
28. Yegneswaran, S., Mesters, R. M., and Griffin, J. H. (2003) *J. Biol. Chem.* **278,** 33312–33318
29. Krishnaswamy, S., Williams, E. B., and Mann, K. G. (1986) *J. Biol. Chem.* **261,** 9684–9693
30. Koppaka, V., Wang, J., Banerjee, M., and Lentz, B. R. (1996) *Biochemistry* **35,** 7482–7491
31. Adams, T. E., Hockin, M. F., Mann, K. G., and Everse, S. J. (2004) *Proc. Natl. Acad. Sci. U. S. A.* **101,** 8918–8923
32. Pellequer, J. L., Gale, A. J., Getzoff, E. D., and Griffin, J. H. (2000) *Thromb. Haemostasis* **84,** 849–857
33. Chen, S. W., and Pellequer, J. L. (2004) *Curr. Med. Chem.* **11,** 595–605
34. Toso, R., and Camire, R. M. (2006) *J. Biol. Chem.* **281,** 8773–8779
35. Nesheim, M. E., Canfield, W. M., Kisiel, W., and Mann, K. G. (1982) *J. Biol. Chem.* **257,** 1443–1447
36. Chothia, C., and Lesk, A. M. (1986) *EMBO J.* **5,** 823–826
37. Cunningham, B. C., Jhurani, P., Ng, P., and Wells, J. A. (1989) *Science* **243,** 1330–1336
38. Fay, P. J., Smudzin, T. M., and Walker, F. J. (1991) *J. Biol. Chem.* **266,** 20139–20145
39. Steen, M., Villoutreix, B. O., Norstrom, E. A., Yamazaki, T., and Dahlback, B. (2002) *J. Biol. Chem.* **277,** 50022–50029
40. Rosing, J., Hoekema, L., Nicolaes, G. A. F., Thomassen, M. C. L. G. D., Hemker, H. C., Varadi, K., Schwarz, H. P., and Tans, G. (1995) *J. Biol. Chem.* **270,** 27852–27858
41. Bukys, M. A., Kim, P. Y., Nesheim, M. E., and Kalafatis, M. (2006) *J. Biol. Chem.* **281,** 39194–39204
42. Brufatto, N., and Nesheim, M. E. (2003) *J. Biol. Chem.* **278,** 6755–6764
43. Orcutt, S. J., and Krishnaswamy, S. (2004) *J. Biol. Chem.* **279,** 54927–54936
44. Sanner, M. F. (1999) *J. Mol. Graph. Model.* **17,** 57–61